Modification of formate stability by alloying: the Cu(100)-c(2 × 2)-Pt system

1999 J. Phys.: Condens. Matter 11 8417

(http://iopscience.iop.org/0953-8984/11/43/304)

J. Phys.: Condens. Matter **11** (1999) 8417–8430. Printed in the UK PII: S0953-8984(99)02470-4

Modification of formate stability by alloying: the Cu(100)–c(2 × 2)–Pt system

J P Reilly, D O'Connell and C J Barnes†

School of Chemical Sciences, Dublin City University, Glasnevin, Dublin 9, Ireland

E-mail: 75020017@raven.dcu.ie

Received 23 April 1999

Abstract. Room temperature deposition of Pt on Cu(100) has been studied by LEED, AES and desorption spectroscopy indicating that sub-monolayer Pt growth at 300 K leads to formation of a poorly ordered c(2 × 2) surface alloy co-adsorbed with Pt microclusters. In contrast to the Cu(100)–c(2 × 2)–Pd system, a high degree of crystalline perfection requires thermal activation which leads to surface Pt atoms switching to second layer sub-surface sites to form a c(2 × 2) underlayer below a copper monolayer.

The presence of Pt in the second layer leads to electronic perturbation of the outermost copper monolayer. Formic acid adsorption on the Cu(100)–c(2 × 2)–Pt sub-surface alloy leads to formation of a formate intermediate with reduced stability relative to clean Cu(100) signalled by a ∼30 K downward shift in the simultaneous CO_2/H_2 evolution. The formate decomposition on the Cu(100)–c(2×2)–CuPt underlayer follows first order decomposition kinetics and the decomposition activation energy is reduced from 119 kJ mol^{-1} (Cu(100)) to 110 kJ mol^{-1} on the CuPt underlayer alloy.

Thicker Pt films with Pt coverages of 1 ML up to 2.5 ML containing significant quantities of Pt in the outermost layer in a local c(2 × 2) environment lead to an additional downward shift in the formate decomposition temperature to 406 K corresponding to a decomposition activation energy of 104 kJ mol^{-1}. This activation energy corresponds to the formate stability on a mixed CuPt bimetallic site. Thus, the surface chemistry of Pt in Cu_3Pt alloys differs significantly from that of pure Pt resulting in a much increased stability for the formate intermediate.

1. Introduction

Miscible bimetallic combinations which form exothermic alloys for which the adsorbed metal has a higher surface energy than the substrate have a tendency to form ordered bimetallic underlayers to minimize the surface free energy [1]. However, the energy gain by forming an ordered underlayer may, in certain cases, be counterweighed by additional strain if there is a considerable size mismatch between substrate and adsorbate and may favour top layer surface alloy formation due to the additional freedom for incorporation of the adsorbate at the vacuum interface. It is often difficult to predict whether it is the ordered bimetallic outer layer or underlayer which dominates the surface alloy metastable phase. Bimetallic surface alloys are of considerable use to probe surface reaction kinetics and dynamics as surface composition can often be more easily controlled than in the case of bulk alloys. It is thus vital for such studies to gain knowledge as to whether adsorbate atoms are located within the outermost layer or occupy sub-surface sites and to quantify the thermal stability of the interface.

† Corresponding author.

0953-8984/99/438417+14$30.00

Copper forms exothermic alloys with the neighbouring transition metal group Ni, Pd and Pt. The bulk phase diagrams for these systems indicate that alloys form throughout the composition range [2]. In the case of Ni a substitutionally disordered fcc alloy is formed while in the cases of Pd and Pt ordered phases also form, particularly around the compositions Cu_3Pt(Pd) and CuPt(Pd) [2].

Of this grouping of surface alloys, the Cu(100)–c(2 × 2)–Pd structure has been and continues to be the most extensively studied. A well developed c(2 × 2) structure is formed at submonolayer Pd coverages upon deposition at 300 K which appears to be best developed at a Pd coverage between 0.5 and 0.8 ML [3, 4]. While early structural work favoured a simple outermost layer alloy of Cu:Pd composition 50:50 [5], more recent work has indicated that the surface layer is heterogeneous with areas of top layer c(2 × 2) CuPd alloy co-existing with areas of pure Cu [6]. A significant quantity of Pd has been shown to reside in the second layer due to capping of c(2 × 2) CuPd top layer domains by ejected copper atoms. Much less is known regarding the surface chemistry of this system with reported work being limited to CO adsorption/desorption which has been extensively probed [7]. Significant changes have been reported in the CO chemisorption bond strength on Pd surface sites in the Cu(100)–c(2 × 2)–Pd surface alloy with desorption maxima being significantly shifted to lower temperature due to modification of the Pd electronic structure towards a d^{10} closed d-band configuration [8]. Significant ongoing interest in this surface alloy remains due to the large changes in the Pd surface electronic structure and reports Pd-induced lattice distortions within the alloy selvedge [9, 10].

The CuPd(Pt) systems are of particular interest catalytically in a range of important reactions including oxidation of CO to CO_2 in automobile catalytic convertors [11] and in a range of hydrocarbon reactions. In particular, the CuPt system has a higher selectivity for hydrocarbon reforming reactions than pure Pt [12]. In addition the CuPd system has relevance to methanol synthesis for which copper is unique in its ability, although Pd is also known to exhibit activity [13, 14].

In contrast to CuPd, little is known of its CuPt counterpart. As Pd and Pt have identical lattice constants and similar electronic properties we may expect similarities between the CuPd and CuPt systems. However, the fact that Pt has a significantly higher surface energy than Pd may also lead to differences both in surface geometry and reactivity. Thus in parallel with a re-examination of the Cu(100)–c(2 × 2)–Pd surface alloy we have undertaken a study of the surface geometric structure and reactivity of the Cu(100)–Pt system and in particular the related Cu(100)–c(2 × 2)–Pt surface alloy. In this case the surface free energy of the adsorbate (Pt) significantly exceeds that of the substrate (Cu) with a surface energy difference of 0.76 J m^{-2} [15]. We illustrate that for low Pt coverages, the chemical ordering has its origin in a mixed CuPt underlayer below a Cu outer monolayer with the bimetallic surface exhibiting a significant 'electronic effect' as monitored by the significantly reduced stability of a formate catalytic intermediate formed by formic acid dosing relative to clean Cu(100). In contrast, higher Pt loadings, while still leading to a well ordered c(2 × 2) alloy interface, have a mixed CuPt top layer. The reactivity of this surface is compared with both clean Cu(100) and the CuPt c(2 × 2) underlayer indicating that significant alteration in the surface chemistry of Pt occurs when incorporated into a copper lattice.

2. Experiment

All measurements were performed in a custom built ion and titanium sublimation pumped ultra-high-vacuum chamber operating at base pressures in the low 10^{-10} Torr regime and will be described in detail elsewhere [16]. The chamber has facilities for quantitative monitoring of

the surface crystallography by low energy electron diffraction via four-grid Vacuum Generators reverse view optics. Quantitative measurements of spot intensities and beam profiles can be made with a Panasonic CCD video camera interfaced to a micro-computer using data aquisition software supplied by Data-Quire corporation (Stony-Brook, NY). The LEED optics also served as a retarding field analyser for surface elemental analysis by Auger electron spectroscopy (AES). A VG Quasar quadrupole mass spectrometer was utilized for residual gas analysis and as a detector for temperature programmed desorption measurements (TPD).

The Cu sample of dimensions $14 \times 10 \times 1.5$ mm was oriented to within 0.5° of the (100) plane (Metals Crystals and Oxides Ltd, Cambridge, UK) and was supplied with four 0.25 mm diameter holes spark eroded into the corners of the sample to aid sample mounting. A fifth 0.25 mm hole was drilled for location of a chromel–alumel thermocouple for temperature measurement. The sample was mounted on a high precision LEED goniometer via suspension between two stainless steel blocks by 0.25 mm diameter tantalum wire passed through the four 0.25 mm holes at the corners of the sample. Heating was achieved by passing a direct current through the tantalum mounting wires allowing temperatures of up to 1000 K to be attained. The sample was cleaned by repeated cycles of argon ion bombardment (3 kV) while annealing at 800 K and was deemed clean when no contaminants could be observed above the AES noise level. At this stage the sample exhibited a sharp p(1×1) LEED pattern with normal incidence $I(V)$ spectra in excellent agreement with literature reports [17].

Platinum was dosed from a home made evaporator consisting of a 0.30 mm tungsten filament around which was tightly wound 0.125 mm Pt wire (Goodfellows Metals: 99.995% purity). The filament was mounted on a feedthrough and shrouded with a stainless steel shield. After thorough outgassing the source provided a slow Pt flux of 0.025 ML min^{-1} at the sample surface which was checked to be homogeneous across the sample. The evaporation rate was calibrated by monitoring the time dependent decrease in the Cu MVV 59/61 eV Auger peak for coverages up to 1 ML and locating the evaporation time which led to a decrease in the MVV signal to 60% of its clean surface value. A decrease of 60% corresponds to that calculated upon assumption of layer-by-layer growth and utilizing an inelastic mean free path of 5.2 Å calculated using the formalism of Seah and Dench [18]. This method obviously relies on the growth mechanism being true layer by layer and will tend to underestimate the true Pt coverage if deviations from layerwise growth occurs. The Auger data were cross checked by quantitatively monitoring the dose time required to obtain a high quality c(2×2) LEED pattern. The LEED intensity maximized at approximately 20% higher evaporation time than that calculated on the basis of AES for formation of a 0.5 ML film.

For desorption experiments formic acid (97% purity, Aldrich chemicals) was further purified by several freeze–pump–thaw cycles prior to dosing. Gas purity was checked using the quadrupole mass spectrometer and dosing performed through an all metal leak valve with exposures measured using an uncalibrated Bayard–Alpert ionization gauge. CO was dosed from ultra-high-purity Messer–Greisheim gas bottles. Desorption spectra were collected in line-of-sight geometry with variable linear heating rates between 1 and 10 K s^{-1}.

3. Results and discussion

3.1. Structural transitions in the Cu(100)–Pt system

Room temperature adsorption of Pt onto the (1×1) surface led initially to a slow increase in the background of the substrate LEED pattern with diffuse low intensity c(2×2) superstructure beams appearing after evaporation times of approximately 9 min. In contrast to the Cu(100)–c(2×2)–Pd system, a good quality c(2×2) was never obtained upon Pt

adsorption at 300 K. Formation of a high quality surface as judged by LEED required thermal activation to temperatures of ∼500 K. Upon cooling to 300 K, a well contrasted c(2 × 2) LEED pattern with intense and sharp half order beams was obtained. In order to examine the optimal Pt coverage and annealing conditions to form a well ordered c(2 × 2) structure, LEED beam profiles were measured as a function of dose time.

Figure 1(a) illustrates selected LEED beam profiles collected at a primary beam energy of 124 eV as a function of Pt evaporation time. The Pt was evaporated at a sample temperature of 330 K with the c(2 × 2) ordering being activated by ramping the temperature to 520 K at a rate of 5 K s^{-1}. The LEED profiles were measured upon re-cooling to a constant temperature of 330 K. The annealing temperature was chosen for its ability to promote surface ordering yet to prevent significant loss of Pt from the outermost bilayer by dissolution into the Cu bulk. The data indicate that the c(2 × 2) becomes visible at an evaporation time of >9 minutes which

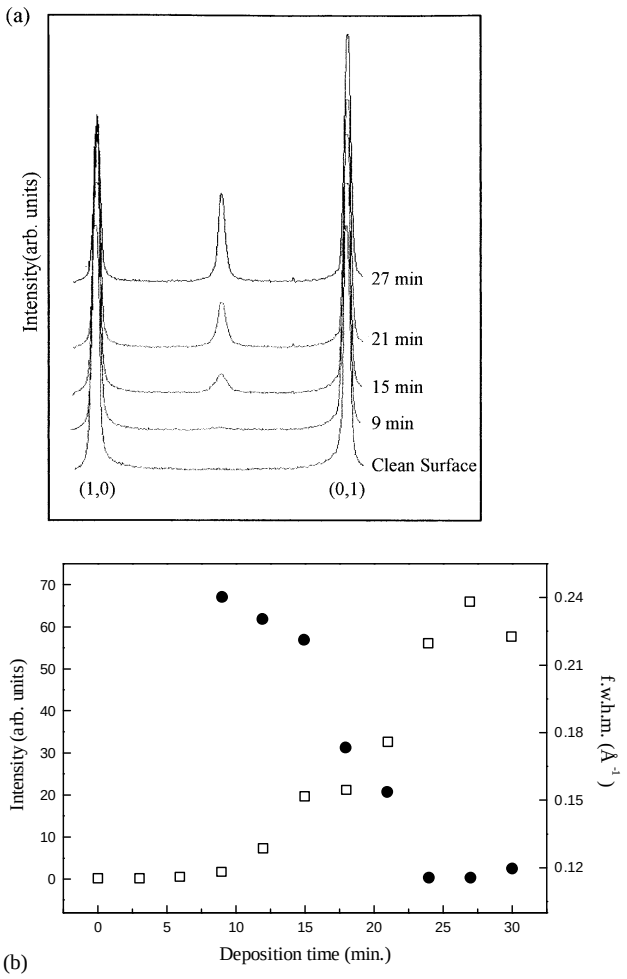

Figure 1. (a) Selected LEED beam profiles measured at 124 eV primary beam energy as a function of Pt coverage. All surfaces were pre-annealed to ∼520 K prior to profile aquisition at 320 K. (b) Variation of the (1/2, 1/2) beam integrated intensity (□) and full width at half maximum (●) with deposition time.

corresponds to a Pt coverage of 0.2 ML based on the Auger calibration. Figure 1(b) illustrates the variation of the $(1/2, 1/2)$ beam intensity and the full width at half maximum (f.w.h.m.) with deposition time. The half-order beam intensity increases up to an evaporation time of 27 minutes (0.61 ML) after which it slowly decreases. The f.w.h.m. decreases for evaporation times between 9 and 25 minutes indicating an increase in the long range order of the c(2×2) superstructure.

The LEED data suggests that at low Pt coverages (<0.2 ML) no two-dimensional islanding of areas of c(2×2) CuPt alloy occurs. Rather it appears that substitution into the copper substrate follows a somewhat random pattern. Ordering on a scale detectable by LEED only becomes apparent at coverages above 0.2 ML at which stage the half-order LEED beams are rather broad and diffuse. Thus, we propose at this critical coverage that small areas of c(2×2) CuPt alloy form until finally at the optimal coverage the half-order beam widths are comparable to those of the clean Cu(100) surface indicating a high degree of long range order. Based on an AES calibration a Pt coverage of 0.6 ML is required to give the 'best' c(2×2).

The temperature dependence of formation of a well ordered surface alloy was investigated by evaporation of a Pt coverage corresponding to the optimal coverage required for c(2×2) formation with the substrate held at 320 K during film growth. The sample was then annealed step-wise to increasingly high temperature and held at temperature for 30 seconds. LEED beam profiles were then aquired upon re-cooling to 320 K. Figure 2(a) illustrates a selection of beam profiles for different annealing temperatures. Figure 2(b) illustrates that a rapid increase in half-order beam intensity is observed between $\sim$400 and 530 K. There is no obvious plateau region and the intensity almost immediately begins to decrease for annealing temperatures above $\sim$540 K with only a very weak c(2×2) remaining upon annealing to 660 K. The increase in beam intensity is accompanied by a decrease in the half-order f.w.h.m. with the minimum half width signifying the optimally ordered surface occurring at $\sim$530 K, the same temperature at which the beam has attained its maximum intensity. Thus we conclude that an 'optimal' c(2×2) surface is formed by annealing a Pt coverage of 0.6 ML briefly to $\sim$530 K and re-cooling to 300 K. It is important to remember that the 'optimal' coverage obtained for c(2×2) formation is the minimum true coverage due to possible deviation from true layerwise growth. Thus, for this system it seems that Pt coverages slightly in excess of the ideal 0.5 ML value are required to bring the c(2×2) to 'maximum perfection' as judged by half-order beam intensities and widths.

The Cu(100)–c(2×2)–Pt system appears to behave significantly differently than the related Cu(100)–c(2×2)–Pd surface alloy where a high quality c(2×2) is observed *directly* after deposition at 300 K. In fact, for the Cu(100)–Pd system recent work indicates that heating to between 400 and 550 K leads to a marked decrease in half-order beam intensity in direct contrast to the increase reported here for the Pt system [19]. We suggest this difference has its origin in the variation in surface thermodynamics for Pd and Pt when deposited on Cu(100). It is well documented that the c(2×2) CuPd alloy formed at 300 K is the result of substitution of Pd into the *outermost* copper monolayer. The outermost layer as mentioned earlier is however heterogeneous due to partial covering of the growing c(2×2) surface alloy by ejected copper atoms. In fact recent work shows that annealing this surface to 500 K leads to capping of the c(2×2) CuPd regions by a copper monolayer and formation of a c(2×2) CuPd underlayer [19] similar to that postulated here for Pt on Cu(100). The lack of formation of a well ordered c(2×2) CuPt alloy on deposition at 300 K cannot be explained by kinetic limitations, as both Pt and Pd have identical atomic size and the arriving Pt atoms have thermal energy well in excess of that of Pd. Formation of an outermost layer surface alloy must be prohibited on thermodynamic grounds due to the higher difference in surface energy (γ) between adsorbate and substrate i.e. γ_{Pt}–γ_{Cu} (0.76 J m^{-2}) relative to γ_{Pd}–γ_{Cu} (0.11 J m^{-2}). Thus, the metastable

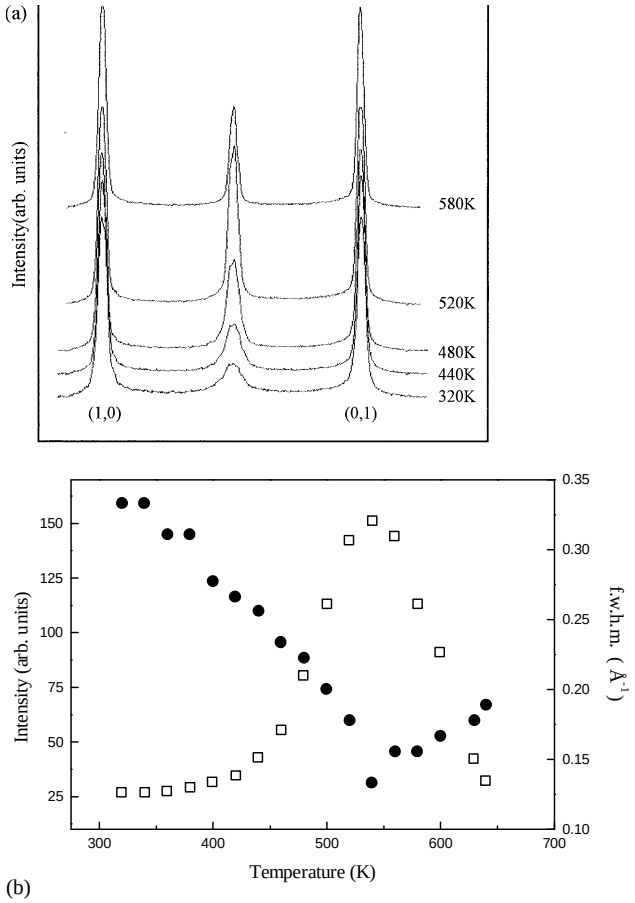

Figure 2. (a) Selected LEED beam profiles measured at a beam energy of 122 eV as a function of annealing temperature for a 0.6 ML Pt film deposited on Cu(100) at 320 K. The profiles were collected after annealing to the quoted temperature for 30 s with beam profiles being collected on re-cooling to ∼320 K. (b) Variation in the (1/2, 1/2) beam integrated intensity (□) and full width at half maximum (●) with annealing temperature.

local free energy minimum in the case of Pt adsorption is likely to be a c(2 × 2) CuPt *underlayer* which has a higher activation energy barrier to formation compared to a top layer alloy due to the correlated atomic motion required. For deposition at 300 K there is insufficient thermal energy for underlayer penetration to go to completion. However, it is clear that some limited alloying does occur as indicated by the observation of weak diffuse c(2 × 2) beams directly upon adsorption.

In order to probe the change in surface stoichiometry which takes place upon annealing, CO desorption spectroscopy was utilized as a probe. Figure 3 illustrates the mass 28 desorption spectra aquired after saturating a 0.5 ML Pt film deposited at 310 K with CO. A large desorption peak was observed (T_p = 415 K) with a low temperature shoulder. Assumption of a pre-exponential factor of 10^{13} s^{-1} and first order desorption kinetics yields a desorption activation energy of 106 kJ mol^{-1}. It is interesting to note that the desorption spectrum obtained resembles that from a metastable Pt(100)–(1 × 1) single crystal surface. Thus, the CO TPD is supportive of the earlier postulation that the major proportion of Pt upon deposition at 300 K is in the

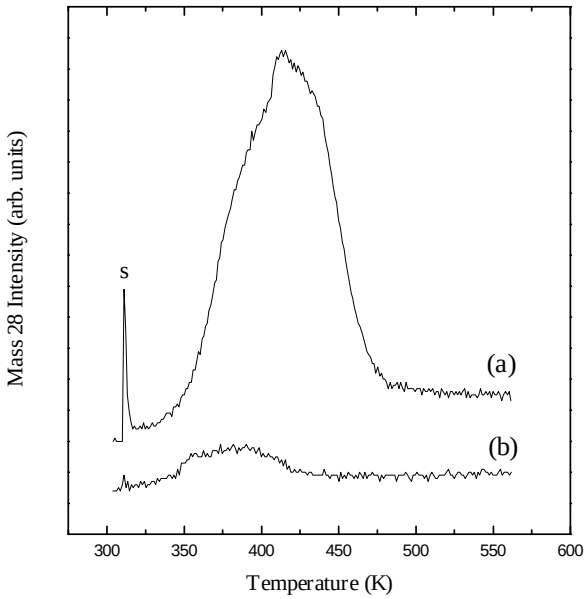

Figure 3. (a) Mass 28 TPD spectra (heating rate 4.5 K s^{-1}) from 0.5 ML of Pt deposited on Cu(100) at 310 K; (b) repeat of (a) performed after re-cooling to 310 K. In both cases the alloy surface was saturated with 100 L of CO at 310 K (s corresponds to the desorption peak from the support wires).

form of a thin Pt(100) pseudomorphic monolayer or Pt(100) crystallites.

In contrast, the same surface when re-saturated with CO at 320 K after the previous activation to 550 K yields only a very weak desorption (figure 3(b)). Clearly a considerable re-distribution of Pt at the interface occurs. It is tempting to simply interpret this result as substitution of Pt atoms into the second layer sites thus forming a c(2×2) underlayer below an outermost copper layer as illustrated in figure 4(a), thus leaving a Cu monolayer outermost which is inert to CO adsorption at 300 K. However, a second possibility which consists of a change to a top layer surface alloy as shown in figure 4(b) is also possible. This second alternative would clearly require a significant alteration in the Pt surface chemistry to an extent that the CO desorption is shifted to well below room temperature. Such an effect is indeed possible as Pt is in a significantly altered local environment with no Pt–Pt nearest neighbours in the surface alloy. However, previous work on a Cu_3Pt bulk alloy in which the top layer consists of a p(2×2) mixed Cu_3Pt layer of composition equal to that of the bulk is not supportive of such a significant downshifting of the CO desorption. This surface, which consists of Pt atoms co-ordinated exclusively to Cu in the outermost layer, exhibits a CO desorption above room temperature ($T_p = 340$–380 K, $\beta = 7$ K s^{-1}), although a significant downshifting of the desorption maximum was observed relative to Pt(111) [20]. As the CO is bound on top sites on the Cu_3Pt alloy [20], it would be unusual to find significantly different desorption behaviour for the Cu(100)–c(2×2)–Pt surface alloy which also consists of isolated Pt atoms available for atop CO bonding if a top layer c(2×2) CuPt alloy were formed.

Hence, the loss of the major CO desorption features is assigned to penetration of the Pt into the second layer of the copper sample to form a CuPt c(2×2) underlayer. It is interesting to note that the small residual CO TPD signal centred at 360 K from the annealed Cu(100)/Pt surface alloy desorbs at similar temperatures to that observed by Schneider *et al* [20] for the

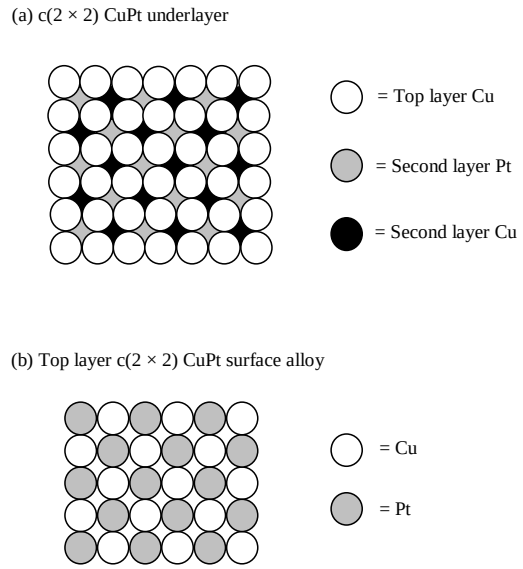

Figure 4. Models for the c(2 × 2) CuPt surface alloy: (a) a c(2 × 2) CuPt underlayer; (b) a mixed outermost layer alloy.

$Cu_3Pt(111)$ single crystal, suggesting that while the majority of Pt does go sub-surface a small number of Pt atoms remain in the outermost layer, although they are minority species with an estimated coverage of <0.05 ML. Thus, it is possible that after annealing small areas of top layer c(2 × 2) CuPt alloy may be present with the exact amount depending of the surface coverage of Pt deposited and the thermal treatment that the overlayer has been subjected to.

The conclusion that annealing for a short time to 530 K leads to penetration of the surface localized Pt to sub-surface sites is in agreement with a low energy ion scattering (LEIS) study of Graham *et al* [21]. These authors noted that for sub-monolayer films prepared by direct deposition had a significant quantity of Pt in the outermost layer. LEIS also indicated a higher Cu concentration in the outermost layer than that expected on the basis of fitting AES results to a layer-by-layer growth mechanism, suggestive of either loss of Pt to sub-surface sites upon deposition or cluster formation. For example, at a Pt coverage of 1 ML (as calibrated by AES) the substrate ion-scattering spectroscopy (ISS) intensity decreases to 40% of its clean surface value. A brief anneal to 525 K was sufficient to reduce the Pt ISS signal to close to zero, indicative of place exchange of Pt into sub-surface sites.

3.2. Effect of surface alloy formation on formate decomposition kinetics

The reactivity of the Cu(100)–c(2 × 2)–Pt alloy was monitored by study of the thermal decomposition of a formate intermediate formed upon dosing of formic acid at room temperature. For adsorption of formic acid on Cu(100) a formate intermediate is formed. Most of the recent structural work is indicative of a geometry in which the formate bridges two nearest neighbour copper atoms [22, 23]. The formate is stable to temperatures above 400 K after which it decomposes, signalled by simultaneous evolution of CO_2 and hydrogen and smaller amounts of molecular formic acid. Figure 5 illustrates the temperature programmed reaction spectroscopy for formate decomposition for saturation formic acid coverage on clean Cu(100) and on a c(2 × 2) surface alloy (formed by pre-annealing a 0.5 ML dose of Pt to

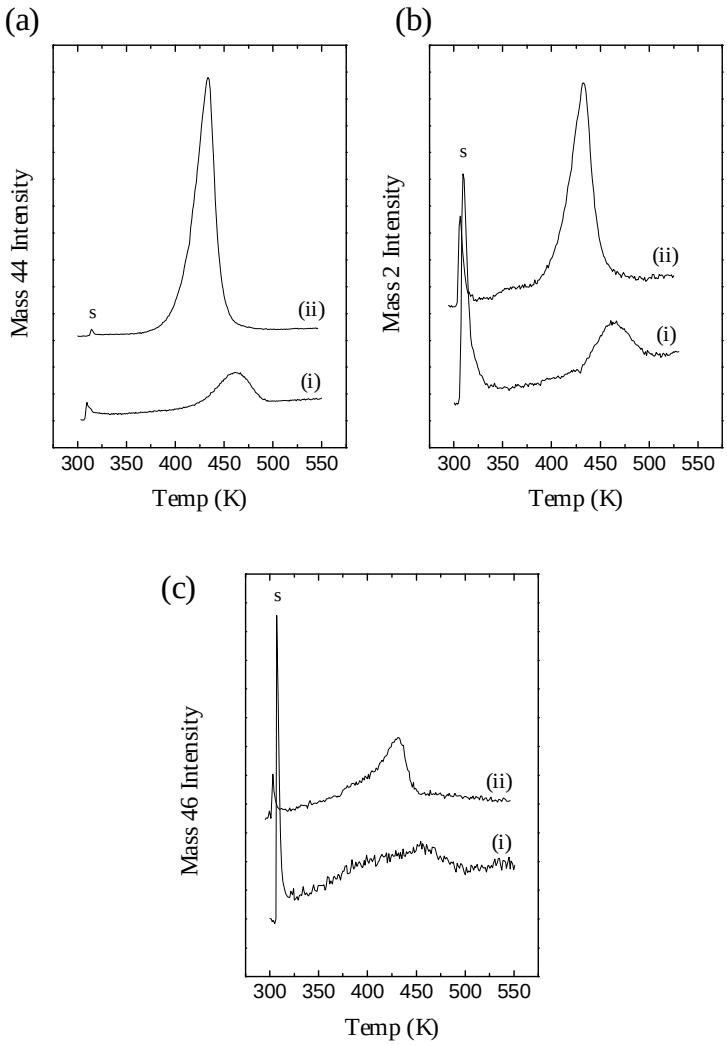

Figure 5. Temperature programmed thermal desorption spectra for saturation coverage of formic acid (HCOOH) on: (i) Cu(100) and (ii) the c(2 × 2) CuPt underlayer alloy, (a) mass 44 (CO_2); (b) mass 2 (H_2); (c) mass 46 (HCOOH). All spectra were recorded with a linear heating rate of 5.0 K s^{-1} (s corresponds to the desorption peak from the support wires).

530 K). Mass 44 (CO_2), mass 2 (H_2) and mass 46 (HCOOH) desorption spectra are illustrated. The clean Cu(100) surface shows simultaneous desorption of CO_2 and H_2 at 461 K, along with a broad molecular desorption peak. Assuming first order formate desorption kinetics and a pre-exponential factor of (10^{13} s^{-1} an activation energy of 119 kJ mol^{-1} is obtained for formate decomposition on clean Cu(100). The corresponding spectra from the c(2 × 2) surface alloy show a significant downward shift of the desorption peak maximum to 432 K, with again a coincident CO_2/H_2 signal. Application of the Redhead equation leads to a decrease in the activation energy for decomposition to 110 kJ mol^{-1}. Interestingly, a decrease in the full width at half maximum from 39 K on clean Cu(100) to 23 K on the c(2 × 2) Pt alloy for CO_2 desorption is observed. Attempts were made to monitor other masses including H_2O (mass 18)

and CO (mass 28), however the only signals seen were coincident with the CO_2/H_2 peaks and were thus assigned to cracking processes of the desorbing CO_2/H_2/HCOOH.

Figure 6 illustrates the effect of heating rate on the CO_2 TPD peak for the Cu(100)–C(2×2)Pt underlayer alloy. The quality of the data was sufficient and the desorption significantly removed from the support peak to allow a full analysis utilizing the leading edge of the peak [24, 25]. Such an analysis in conjunction with heating rate variation data yielded a conclusion that the decomposition occurs via first order decomposition kinetics on the alloy surface with an activation energy for decomposition of 116($\pm$3) kJ mol^{-1} and a pre-exponential factor of 4.2($\pm$4.8) $\times$ 10^{13} s^{-1} from the 4.83 K s^{-1} heating rate, in reasonable agreement with the value obtained by the Redhead method. A leading edge Arrhenius plot for the 4.83 K s^{-1} heating rate is shown in figure 6(b).

As the c(2×2) structure corresponds to a mixed CuPt underlayer with a copper monolayer outermost, then the decreased formate stability must be due to an 'electronic effect' of the

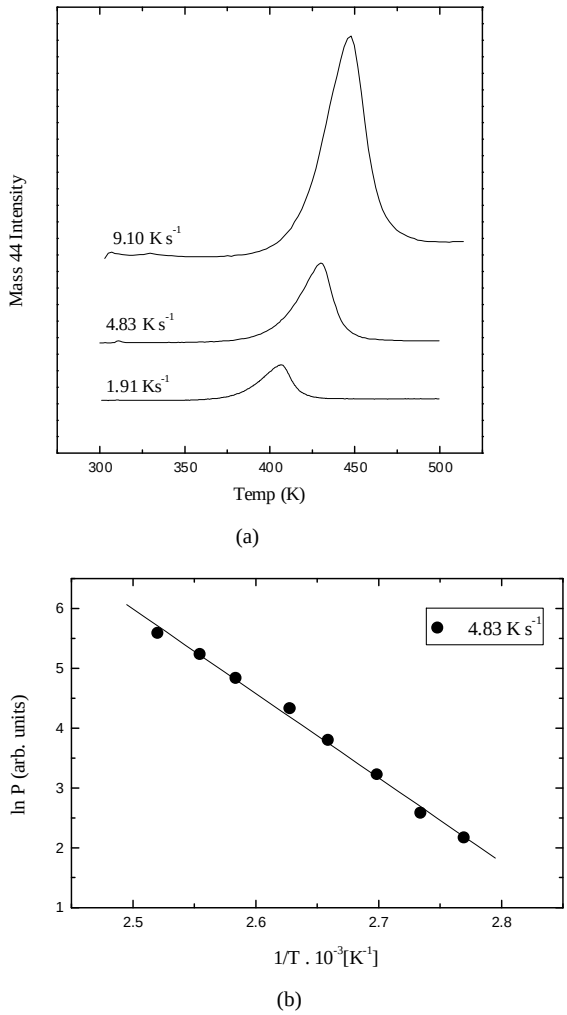

Figure 6. (a) Effect of heating rate on the mass 44 (CO_2) peak for the c(2×2) CuPt underlayer alloy; (b) an example of an Arrhenius plot utilizing the leading edge analysis method.

second layer Pt on the top layer Cu atoms if we assume that the formate adopts a similar geometry to that found on clean Cu(100). While there have been no past studies of the effect of Pt on the reactivity of copper surfaces with respect to formate decomposition, the CuPd system has received considerable attention. Newton and Bowker [26] have studied the effect of a sub-surface p(2 × 1) CuPd underlayer below a Cu rich top layer for a $Cu_{0.85}Pd_{0.15}(110)$ bulk alloy. These authors report using the complete analysis approach [24, 25] that sub-surface Pd in a 50:50% local composition leads to a destabilization of the formate intermediate from a decomposition activation energy of 136.4(±3) kJ mol^{-1} on clean Cu(110) to 125(±3) kJ mol^{-1} on the alloy surface, while a Redhead analysis also leads to a Pd induced destabilization, a smaller (2%) decrease in decomposition activation energy is indicated. This 6% decrease in activation energy is similar in magnitude to that on the Cu(100)–c(2 × 2)–Pt underlayer surface (slightly higher at 7%), although the absolute activation energies of Newton and Bowker are somewhat higher than those obtained in this work. Table 1 illustrates formate decomposition activation energies for a range of Cu, Pd and CuPd alloy surfaces calculated using the Redhead method along with results of this study on Cu(100)–Pt. We believe the Redhead method, although not exact, is the best way to compare the sets of data taken in different laboratories. The coverage dependence of the formate stability was also investigated on the Cu(100)–c(2 × 2)–Pt underlayer by dosing 0.1 L of formic acid. A leading edge and Redhead analysis indicated that within the accuracy of either analyses, no coverage dependent changes in the stability of the formate species occurs.

Table 1. Comparison of the activation energy for formate decomposition (E_{act}) on various surface alloys. The values were calculated utilizing the Redhead approximation with a pre-exponential factor of 10^{13} s^{-1}.

Substrate	β/K s^{-1}	T_{max}/K	E_d/kJ mol^{-1}	Ref.
Pd(110)	3.0	237	60	[31]
Cu(110)	1.8	445	118	[27]
1 ML Pd/Cu(11)	1.2	430	115	[27]
4 ML Pd/Cu(110)	1.5	363	96	[27]
CuPd[85:15](110) (2 × 1)	2.65	445	116	[32]
CuPd[50:50](110)	2.5	346	90	[33]
Cu(100)	5.0	461	119	This work
Cu(100)–c(2 × 2)–Pt	5.0	432	110	This work
Cu(100)–c(2 × 2)–Pt*	5.0	406	104	This work

* mixed CuPt layer.

Reilly *et al* [27] have recently shown that, for CuPd systems formed by sublimation of Pd onto a Cu(110) surface, the stability of the formate intermediate may be altered depending on the Pd loading and thermal processing undergone by the system. In particular, from copper capped p(2 × 1) surfaces of similar local geometry/composition to the bulk alloy of Newton and Bowker, a similar de-stabilization of the formate stability is encountered as that previously reported [26].

The mechanism of formation of a c(2 × 2) CuPt underlayer requires further brief comment. Substition of 0.5 ML of Pt into the outermost layer of the Cu(100) substrate naturally requires that 0.5 ML of Cu is expelled. These copper atoms must then reside above the surface with the natural conclusion that a somewhat heterogeneous surface will initially arise with large areas consisting of an outermost copper monolayer above a c(2 × 2) mixed CuPt layer. As the Pt c(2 × 2) films for Pt coverages of 0.5 ML yield no evidence of a high temperature desorption state reflecting coincident CO_2/H_2 desorption at 461 K (CO_2 peak from clean Cu(100)), we may conclude that we have indeed deposited the minimum Pt coverage (0.50 ML) required to

form a homogeneous c(2 × 2) second layer. Hence, the additional 0.5 ML of Cu required to fully cap the c(2 × 2) CuPt underlayer must be transported from step edges. Additional Pt over and above that required to form the mixed underlayer is then likely to be located within the outermost layer as it is unlikely that a brief anneal to 520 K will provide sufficient activation energy to transport a significant number of Pt atoms into the copper bulk, possibly explaining the small residual CO desorption (figure 3). The lack of formate decomposition at ∼400 K and the small full width at half maximum of the fomrate decomposition is thus clear evidence that no areas of un-alloyed clean Cu(100) surface remain i.e. a rather homogeneous c(2 × 2) underlayer forms.

In order to investigate the possibility of stabilising Pt in the outermost layer, interfaces of higher Pt loading were produced. Graham *et al* [21] has observed that thicker films (>1 ML) annealed to 525 K have a significant Pt content in the outermost layer. For example, a Pt coverage of 3 ML deposited at 300 K yields a pure Pt surface as analysed by ISS. Annealing to 525 K leads to a large reduction in the Pt signal and re-apearance of a Cu ISS signal inkeeping with a mixed CuPt outermost layer. Belkhou *et al* [28] have reported that deposition of thicker Pt films followed by annealing to 575 K lead to a well ordered c(2 × 2) alloy with a mixed CuPt outermost layer in agreement with the ISS work of Graham *et al* [21]. Utilizing the technique of surface core level shift spectroscopy Belkhou *et al* observed that the Pt 4f core level had a significant surface component which the authors ascribed to Pt atoms within a mixed *outermost* CuPt layer above an alloyed interface of average composition Cu_3Pt. Thus while it would appear that in the sub-monolayer regime the mixed CuPt layer prefers to be sub-surface at higher Pt loading the role is reversed with the mixed layer being outermost.

Figure 7 illustrates the mass 44, mass 2 and mass 46 TPD spectra for Pt films of thickness 0.5, 1, 1.5 and 2.5 ML. The 1 ML film illustrates strong simultaneous CO_2/H_2 desorption at 426 K. The LEED pattern in this case remained an excellent c(2 × 2). The CO_2 desorption peak has a particularly narrow half-width (11 K) at Pt coverages of 1.5 ML, indicative of a highly homogeneous surface. Again this surface exhibits an excellent c(2 × 2) LEED pattern. The simultaneous CO_2/H_2 evolution is further downshifted to 406 K. As the 1.5 ML c(2 × 2) surface has a mixed CuPt layer outermost we thus have direct evidence of a significant alloying induced change in the Pt surface chemistry. Madix [29] has shown that on Pt(110) the maximum rate of formate decomposition occurs below room temperature at ∼250 K. Thus, while the mixed CuPt surface does show a formate stability intermediate between that of Pt and Cu, the surface chemistry remains more similar to that of Cu(100). This is perhaps not surprising given that a c(2 × 2) CuPt outermost layer requires formate to bond at *mixed* CuPt sites if it is to bridge two nearest neighbour atoms in the outermost layer. The UPS work of Schneider *et al* [20] along with band structure calculations of Banhart *et al* [30] indicate that for dilute CuPt alloys the platinum atoms adopt a d^{10} filled d-band configuration. This may be expected to passify reactivity towards formate decomposition and yield properties more similar to those encountered on copper. Finally, in the case of 2.5 ML of Pt the LEED pattern degraded substantially to a high background c(2 × 2). The CO_2 and H_2 peaks are substantially broadened relative to the 1.5 ML film, indicating considerable surface heterogeneity. The simultaneous CO_2/H_2 desorption is centred at 412 K with significant desorption at lower temperatures, indicative of regions of the surface containing alloyed Pt in the outermost layer with varying degrees of Pt–Pt nearest neighbour bond formation. This should lead to a gradual destabilization of formate on Pt rich areas of the surface and the concomitant broadening in the formate decomposition [27]. Nevertheless, the fact that the surface chemistry has not crossed over to Pt-like behaviour clearly illustrates that large regions of pure Pt clusters are still not present at the surface.

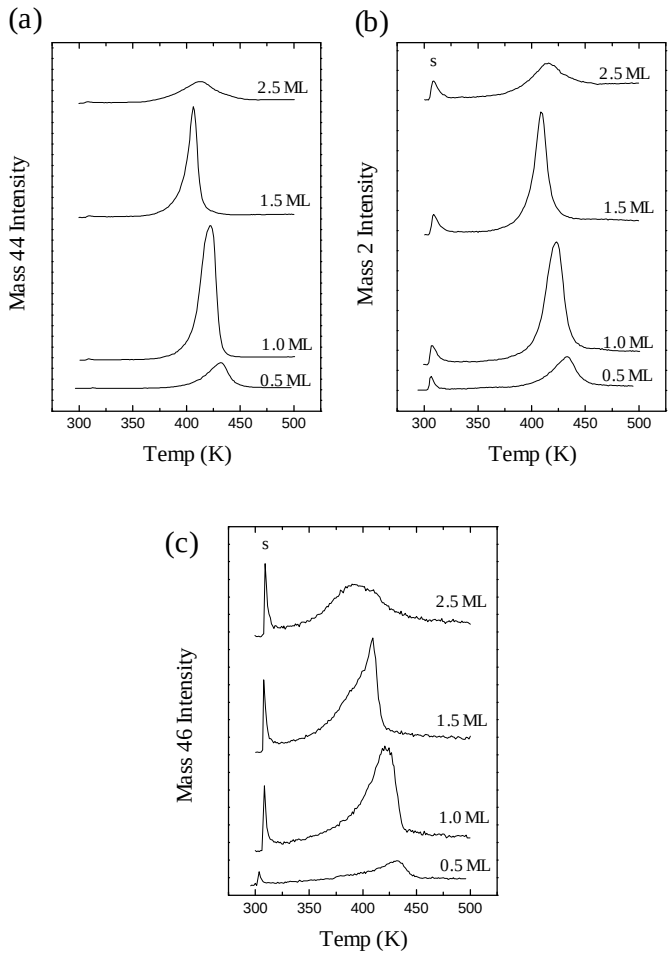

Figure 7. Effect of higher Pt loadings on the formate decomposition kinetics: (a) mass 44 (CO_2); (b) mass 2 (H_2); (c) mass 46 (HCOOH). All surfaces were pre-annealed to 530 K prior to dosing to saturation HCOOH coverage (10 L) (s corresponds to the desorption peak from the support wires).

4. Conclusions

Copper–platinum surface alloys have been formed by deposition of Pt onto Cu(100) and structural transitions as a function of Pt coverage and thermal processing have been followed by LEED and desorption spectroscopy. Adsorption of Pt leads to the formation of a c(2×2) surface alloy. Formation of a well ordered surface requires thermal activation to 530 K and Pt coverages slightly in excess of 0.5 ML while annealing above this temperature leads to slow dissolution of Pt into the bulk. Combination of AES analysis and CO TPD strongly suggests that a surface subject to a brief anneal to temperatures in excess of 500 K results in the formation of a c(2×2) CuPt *underlayer* below a Cu(100) surface layer.

Platinum exerts a considerable 'ligand' effect on the outermost copper monolayer destabilizing the formate intermediate which undergoes a first order decomposition with an activation energy of 110 kJ mol^{-1}, a 7% decrease in the formate decomposition activation energy relative to Cu(100). Higher Pt coverages lead to formation of a c(2×2) overlayer

with a mixed CuPt layer outermost. On these surfaces formate decomposition is further destabilized with a decomposition activation energy of 104 kJ mol^{-1} (a 13% decrease in the activation energy barrier relative to clean Cu(100)). Alloying platinum with copper leads to significant chemical modification of the chemistry of Pt sites; however this 'electronic effect' is mixed with a geometric effect due to the mixed CuPt nature of the site (if formate remains bridging two nearest neighbour metal atoms) on the high Pt loading CuPt interface.

Acknowledgments

We would like to thank FORBAIRT (now Enterprise Ireland) for assistance in partially funding the research reported here. We also acknowledge the participation of Dr Tony Cafolla and Mr Paul Quinn in the early stages of this work.

References

[1] Bardi U 1994 *Rep. Prog. Phys.* **57** 939
[2] Hansen M 1958 *Constitution of Binary Alloys* 2nd edn (New York: McGraw-Hill)
[3] Graham G W 1986 *Surf. Sci.* **171** L432
[4] Smith G C, Norris C and Binns C 1981 *Vacuum* **31** 523
[5] Lu S H, Wang Z Q, Wu S C, Lok C K C, Quinn J, Li Y S, Tian D, Jona F and Marcus P M 1988 *Phys. Rev.* B **37** 4296
Wu S C, Lu S H, Wang Z Q, Lok C K C, Quinn J, Li Y S, Tian D, Jona F and Marcus P M 1988 *Phys. Rev.* B **38** 5363
[6] Valden M, Aaltonen J, Pessa M, Gleeson M and Barnes C J 1994 *Chem. Phys. Lett.* **228** 519
[7] Pope T D, Griffiths K and Norton P R 1994 *Surf. Sci.* **306** 294
[8] Rao R S, Bansil A, Asonen H and Pessa M 1984 *Phys. Rev.* B **29** 1713
[9] Bowker M, Newton M, Francis S M, Gleeson M and Barnes C J 1994 *Surf. Rev. Lett.* **1** 569
[10] Newton M, Bowker M, Weightmann P, Gleeson M and Barnes C J *Phys. Rev. Lett.* submitted
[11] Toolenaar F J C H, Stoop F and Ponec V 1983 *J. Catal.* **83** 1
[12] de Jonste H C and Ponec V 1980 *J. Catal.* **63** 389
[13] Poutsma M L, Elek L F, Ibarbia R A, Rich A B and Rabo J A 1978 *J. Catal.* **52** 152
[14] Ponec V 1992 *Surf. Sci.* **272** 111
[15] Tyson W R and Miller W A 1977 *Surf. Sci.* **62** 267
Mezey L Z and Giber J 1982 *Japan. J. Appl. Phys.* **21** 1569
[16] Barnes C J, O'Connell D and Gleeson M, in preparation
[17] Davis H L and Noonan J R 1982 *J. Vac. Sci. Technol.* **20** 842
[18] Seah M P and Dench W A 1979 *Surf. Interface Anal.* **1** 2
[19] Shamayleh E Al and Barnes C J, work in progress
[20] Schneider U, Busse H, Linke R, Castro G R and Wandelt K 1994 *J. Vac. Sci. Technol.* A **12** 2069
Castro G R, Schneider U, Busse H, Janssens T and Wandelt K 1992 *Surf. Sci.* **269/270** 321
[21] Graham G W, Schmitz P J and Thiel P A 1990 *Phys. Rev.* B **41** 3353
[22] Woodruff D P, McConville C F, Kilcoyne A L D, Lindner T, Somers J, Surman M, Paolucci G and Bradshaw A M 1988 *Surf. Sci.* **201** 228
[23] Mehandru S P and Anderson A B 1989 *Surf. Sci.* **219** 68
[24] Habenschaden E and Kuppers J 1984 *Surf. Sci.* **138** L147
[25] King D A 1975 *Surf. Sci.* **47** 384
[26] Newton M A and Bowker M 1994 *Surf. Sci.* **307** 445 and references therein
[27] Reilly J, Barnes C J, Price N J, Poulston S, Stone P and Bowker M *J. Phys. Chem.* submitted
[28] Belkhou R, Thiele J and Guillot C 1997 *Surf. Sci.* **377** 948
[29] Madix R 1981 *Surf. Sci.* **102** 542
[30] Banhart I, Weinberger P and Voitlander J 1989 *Phys. Rev.* B **40** 12 097
[31] Aas N, Li Y and Bowker M 1991 *J. Phys.: Condens. Matter* **3** 1
[32] Newton M A, Francis S M, Li X, Low D and Bowker M 1991 *Surf. Sci* **259** 45
[33] Holroyd R *PhD Thesis* Reading Catalysis Centre, University of Reading, UK